Iran J Sci Technol Trans Sci (2017) 41:599–607
DOI 10.1007/s40995-017-0307-9

RESEARCH PAPER

The Crystal Structure of the Ba-Hexacelsian Phases Doped with Ca^{2+} and Pb^{2+}

A. Radosavljevic-Mihajlovic[1] · S. Radosavljevic[1] · J. Stojanovic[1]

Received: 29 June 2015 / Accepted: 19 October 2016 / Published online: 5 October 2017

Abstract The ion-exchange procedure is used for doping the Ba-hexacelsian structure with Ca^{2+} and Pb^{2+} cations. The hexacelsian doped with Ca^{2+} has a composition of $Ba_{0.64}Ca_{0.36}Al_2Si_2O_8$, and hexacelsian doped with Pb^{2+} has a composition $Ba_{0.9}Pb_{0.1}Al_2Si_2O_8$. The crystal structure of both doped hexacelsians was refined by Rietveld refinement procedure. The crystal structure of Ca-hexacelsian is refined in the space group $P\bar{3}c1$, and results indicate ordering distribution of Si and Al (unit cell parameters is $a = 5.2995$, $c = 15.594$ Å and agreement factors: $R_{exp} = 15.3$ $R_p = 19.9$, $R_{wp} = 19.0$, $R_B = 15.0$ $R_F = 4.08$). Structural model for Pb-hexacelsian samples is described in the space group $P6_3/mcm$ with disorder distribution Si/Al (unit cell parameter is $a = 5.2973$, $c = 15.591$ Å and agreement factors $R_{exp} = 21.5$ $R_p = 21.5$, $R_{wp} = 19.0$, $R_B = 5.74$ $R_F = 4.08$). The results of Rietveld refinements indicate that Ca^{2+} and Pb^{2+} cations are incorporated into hexacelsian structure in different position.

Keywords Rietveld refinement · Thermal treatment · Structure of doped Ca-hexacelsian · Structure of Pb-doped hexacelsian

✉ A. Radosavljevic-Mihajlovic
amihajlovic332@gmail.com

[1] Institute for Technology of Nuclear and Other Mineral Raw Materials, Franshe D'Epere 86, 11000 Belgrade, Serbia

1 Introduction

According to crystal chemical classification, alkaline earth diphylloaluminosilicates belongs to the unbranched phyllosilicate structural type (Libay 1985). The hexacelsian ($BaAl_2Si_2O_8$) is an important thermo-stable ceramic material because it has low thermal expansion and good dielectric properties. In recent years, the hexacelsians doped with different cations can be used as new ceramic materials. These doped materials have broad applications, such as phosphors for plasma display panels (PDP), field-emission displays, and fluorescence lamps (Kim et al. 2000; Talin et al. 2001). The basic characteristic of diphyllosilicate structure type is the presence of successive double $Al_2Si_2O_8$ tetrahedral sheets separated by Ba^{2+} cation layers. Each $Al_2Si_2O_8$ sheet consists of an upward and downward oriented TO_4 ($T = Si^{4+}$, Al^{3+}) tetrahedral sub-layer bridged via O_1 atoms (Ito 1950; Yoshiki and Matsumoto 1951; Takéuchi 1958; Takéuchi and Donnay 1959; Kremenović et al. 1997).

The space group for hexacelsian with chemical formula $M^{2+}Al_2Si_2O_8$ is P6/mmm. The M-cation is located on 1*a* sites, $Al_{0.5}Si_{0.5}$ on 4 h sites and oxygens on 2*d* and 6*i* sites in this structure (Tabira et al. 2000). Tabira et al. investigated the structure of pure and Cs-, Rb-doped Ba-hexacelsian, and it was found that the structure of Cs- and Rb-doped Ba-hexacelsian is present with extremely strong and characteristic diffuse intensity distribution along [$-h$ h o l] directions of reciprocal space (Tabira et al. 2000). Isaacs (1971) observed the process of luminescence in Eu^{2+}, Sm^{2+}- and Sm^{3+}-doped hexacelsian. Ishihara et al. (Ishihara et al. 1997, 1998) investigated triboluminescence and photoluminescence properties of hexacelsians doped with the Eu^{3+}, Sm^{2+}, Sm^{3+}, Yb^{2+} or Ce^{3+}. The authors suggested that the Sm^{2+} ions could replace Ba^{2+} ions

which occupy the sites with inversion symmetry. They proposed a space group (SG) of *P*6/mmm for the doped hexacelsian structure and suggested that the Eu^{3+} exchange exclusively the Ba^{2+} site that is placed in the crystallographic site with the $D_{6\ h}$ symmetry. Colomban et al. (2000) published the results of Li-doped hexacelsian polymorphs and this author did not clearly indicate whether Li enters in the structure of hexacelsian. They could replace barium ions, leading to Ba deficiency, but also occupy tetrahedra sites, replacing Al or Si cations. Kremenović et al. (Kremenovic et al. 2003) investigated the crystal structure of non-doped and Eu^{3+}- doped hexacelsian$_{LTA}$. The structure was refined in the SG $P6_3/mcm$ assuming disorder distribution of the Si^{4+} and Al^{3+} and Eu^{3+} that replace only Ba^{2+}. In the Eu^{3+}-doped sample, a large number of defects were indicated in the structure. kim et al. (2006) solved the crystal structure of the Ba-hexacelsian doped Eu^{2+} ions. When Eu^{2+} ions are incorporated into the crystal structure of hexacelsian, Eu^{2+} ions may substitute at all cationic sites, Ba^{2+}, Al^{3+} and Si^{4+}. The Rietveld refinement was refined in the SG $P\bar{3}$ and carried out under the assumption that Eu^{2+} ions substituted only Ba^{2+} ions. Sinha et al. (2009) confirmed the structural model proposed by Kremenovic et al. (2003), based on investigated it is clear that Eu^{2+} only occupies the barium site.

Nedić et al. (2007) investigated the structure of Ba and Sr hexacelsian doped with Yb^{3+} ions. The structure of Ba-hexacelsian is refined into the SG $P\ \bar{3}$, while the structure of Sr hexacelsian doped with Yb^{3+} is refined into the SG $P\bar{3}c1$. The results of Rietveld refinements clearly indicate that Yb^{3+} ions are incorporated into the hexacelsians structure. Dondur et al. (2005) investigated the role and influence of Li^+ and Na^+ ions dopants on reversible α-to β-HC transition. The results show that the ions are incorporated in HC and influence polymorphic transformation of HC into MC. Based on the literature data (Colomban et al. 2000; Kremenovic et al. 2003; Nedic et al. 2007; Dondur et al. 2005), it is still unknown where the dopants are incorporated in the hexacelsian structure. In this work, Ba-hexacelsian doped with Ca^{2+} and Pb^{2+} ions was synthesized using zeolites as a starting material using ion-exchange procedure. The main goal of this work was to determine the crystal structures of Ba-diphylloaluminosilicate phases doped with Ca^{2+} and Pb^{2+} cations.

2 Experimental Part

The Ba-hexacelsian (HC) compound was synthesized by ZTIT procedure described elsewhere (Dyer 1998; Radosavljevic-Mihajlovic et al. 2012). Sodium zeolite with LTA (type A; Si/Al = 1.00) framework, manufactured by Union Carbide Co., was used as starting material. Prepared HC sample was used as the starting material for further chemical modification (Table 1). The ion-exchange procedure was used for doping the Ba-hexacelsian structure with Ca^{2+} and Pb^{2+} ions. The following procedure (Dyer 2001) was performed for cation exchange of HC sample: 3 g of initial HC obtained in the above described manner was were treated with a 0.90 dm^3 of 0.5 M solution of calcium chloride and a second sample was treated in 0.5 M solution of $PbCl_2$ (solid/liquid ratio = 1/30) in autoclave near constant temperature of 180 °C. The solid filtrate phase was separated from the liquid through filtration and again treated with the new exchange solution (0.90 dm^3) for a total of ten times. After 7 days, the sample was noted as 1HC-Ca, HC-Pb and after 14 days the sample was noted as 2HC-Ca. The ion-exchanged samples were washed and dried. The presence of Na^+, Ba^{2+}, Ca^{2+} and Pb^{2+} in samples was checked by atomic absorption spectrophotometry (AAS) using a Varian Spectra AA55 Spectrometer. Using EDAX method, the presence of Si, Al, Na, Ca, Pb and Ba cations in the synthesized compounds was controlled. The results of chemical analysis are shown in Table 1.

The X-ray powder diffraction (XRPD) patterns of doped samples were obtained on a Philips PW-1710 automated diffractometer using a Cu tube operated at 40 kV and 30 mA. The instrument was equipped with diffracted beam curved graphite monochromatic and a Xe-filled proportional counter. The XRPD data were refined to the both structure models with the aid of computer program Fullprof (Rodriguez-Carvajal and Roisnel 1998). For a Rietveld profile fitting method, the XRPD data were collected by using the step scanning mode in the range of Bragg angle $2\Theta = 4^{\circ}$–135° at each 0.02 step counting for 12.5 s. The divergence and receiving slits were fixed at 1^{o} and 0.1 mm, respectively. All the XRPD patterns measurements were performed ex situ at the room temperature in a stationary sample holder.

3 Results and Discussion

3.1 Chemical, XRPD and SEM/EDS Analysis

The results of EDAX and AAS chemical analysis of ion-exchanged samples of HC used in this study are presented in Table 1.

These data clearly show that the initial Na-LTA zeolite is nearly completely exchanged to Ba^{2+} cations. The residue of Na_2O weight percent could be neglected in chemical formulas of Ca-substituted phases presented in Table 1. It follows from the discussed results that these compounds are stoichiometric which can be proved from

Table 1 Chemical composition of hexacelsian (HC) doped with Ca^{2+} (1HC-Ca, 2HC-Ca) and Pb^{2+} (HC-Pb) and its chemical formula

Samples	Elements (%)						Chemical formula
	SiO_2	Al_2O_3	NaO	BaO	CaO	PbO	
HC	34.89	29.67	0.05	33.70	–	–	$BaAl_2Si_2O_8$
1HC-Ca	34.90	29.67	–	28.45	5.25	–	$Ba_{0.64}Ca_{0.36}Al_2Si_2O_8$
HC-Pb	34.90	29.81	–	28.82	–	4.98	$Ba_{0.9}Pb_{0.1}Al_2Si_2O_8$
2HC-Ca	37.54	31.38	–	18.22	13.00	–	$Ba_{0.37}Ca_{0.63}Al_2Si_2O_8$

Al/Si ratio, i.e., they were inherited framework cations ratio of initial zeolite. A basis to chemical results the ion-exchanged $Ba^{2+}\rightarrow Ca^{2+}$ and $Ba^{2+}\rightarrow Pb^{2+}$ in hexacelsian not completed. The results of chemical analysis, Table 1, show that the content of CaO in HC sample exchanged after 7 days was 6.70 wt% and after 14 days was 13%. The content of PbO in HC-Pb sample is 10%.

The XRPD patterns and evolution of crystal morphology of starting (HC) and ion-exchanged hexacelsian (1HC-Ca, 2HC-Ca and HC-Pb) are shown in Fig. 1. The main morphological feature of starting hexacelsian (HC) is the presence of cubic crystal formation. However, the discussed cubic morphology is kept at higher temperatures where amorphous substance (Ba-LTA zeolite) is recrystallized into HC phase. This phenomenon is known in mineralogy and could be classified as pseudomorphos HC obtained from Ba-LTA crystals, which is visible in Fig. 1.

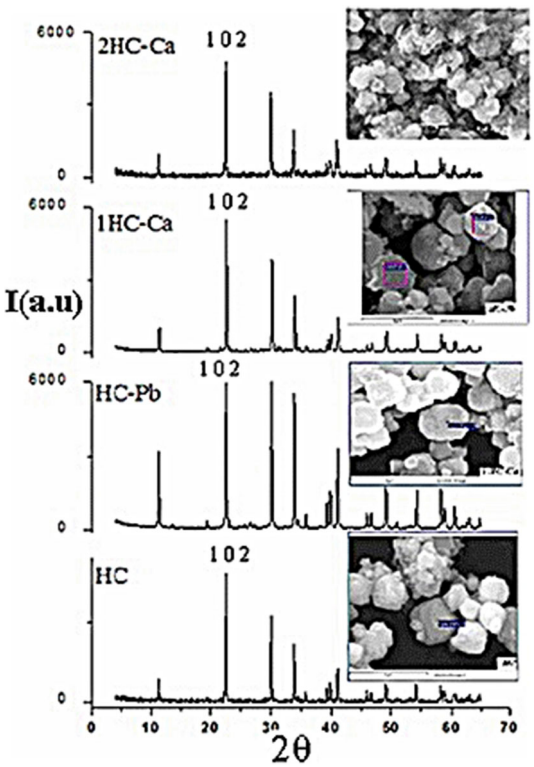

Fig. 1 The comparative XRPD diagrams and SEM images of starting (HC) and ion-exchanged hexacelsian (HC-Pb, 1-HC-Ca, 2HC-Ca)

Observed cubic forms of HC phase remain stable during the process of ion exchange ($Ba^{2+}\rightarrow Ca^{2+}$ and $Ba^{2+}\rightarrow Pb^{2}$), the sample 1HC-Ca and HC-Pb, Fig. 1. The crystal morphology of sample 2HC-Ca is presented with diffuse rounded edges.

The XRPD pattern of doped hexacelsian in Fig. 1 shows changes of diffraction maximum, displacements of *d*–values [the reflection (102) in HC sample $d = 3.98$, 1-HC-Ca $d = 3.89$, HC-Pb $d = 3.89$, 2-HC-Ca $d = 3.83$]. The parameter of unit cell of started and doped hexacelsian is presented in Table 2.

We can conclude that with the increasing content of Ba^{2+} in the structure of hexacelsian the volume of the unit cell is in growth (Fig. 2).

Based on the chemical analysis the content of Ca in sample 1 HC-Ca is 3.75% and content of Pb in HC-Pb is 4.62% (Table 2). The changes in crystal chemical composition lead to modification of the unit cell parameters in structure of doped hexacelsian. The Pb-hexacelsian crystallizes in the space group $P6_3/mcm$, and Ca- hexacelsian in the space group $P\bar{3}c1$. The higher content of Ca ions in the hexacelsian structure of 9.29% leads to a decrease of unit cell volume.

The ion-exchanged samples were thermally treated at a temperature of 1100 °C/2 h to observe the thermal stability of the ion-change hexacelsian. The ion-exchanged samples were thermally treated at a temperature of 1100 °C/2 h, to observe the thermal stability of the ion-change hexacelsian. The spontaneous thermally induced transformation of hexacelsian to celsian phase needs prolonged heating at temperatures higher than 1500 °C for several hours. Several authors have observed the influence of various dopants on the acceleration of celsian nucleation (Colomban et al. 2000; Ferone et al. 2005; Dondur et al. 2005; Dondur, et al. 2008). According to these results, dopants have a significant role in acceleration of hexacelsian → celsian transformation process. The XRPD patterns of thermal-treated samples in 1100 °C/2 h of starting (HC) and ion-exchanged hexacelsian (1HC-Ca, 2HC-Ca and HC-Pb) are shown in Fig. 3.

According to the XRPD patterns (Fig. 3), the samples (HC, 1HC-Ca and HC-Pb) were transformed into celsian. The samples of ion exchanged (1HC and HC-Ca–Pb) show a higher degree of crystallinity, relative to the starting HC. In this temperature, the sample 2HC-Ca was transformed into the gehlenite mineral with tetragonal symmetry, with

Table 2 The parameter of unit cell and space group of started and doped hexacelsian

Samples	Chemical formula	Space group	a (Å)	c (Å)	V (Å)^3
HC	$BaAl_2Si_2O_8$	$P6_3/mcm$	5.299 (1)	15.582 (2)	379.0 (1)
HC–Pb	$Ba_{0.9}Pb_{0.1}Al_2Si_2O_8$	$P6_3/mcm$	5.305 (2)	15.585 (2)	378.0 (1)
1HC-Ca	$Ba_{0.64}Ca_{0.32}Al_2Si_2O_8$	$P\bar{3}c1$	5.282 (4)	15.553 (3)	375.5 (2)
2HC–Ca	$Ba_{0.37}Ca_{0.63}Al_2Si_2O_8$	$P\bar{3}c1$	5.180 (2)	15.507 (1)	365.5 (1)

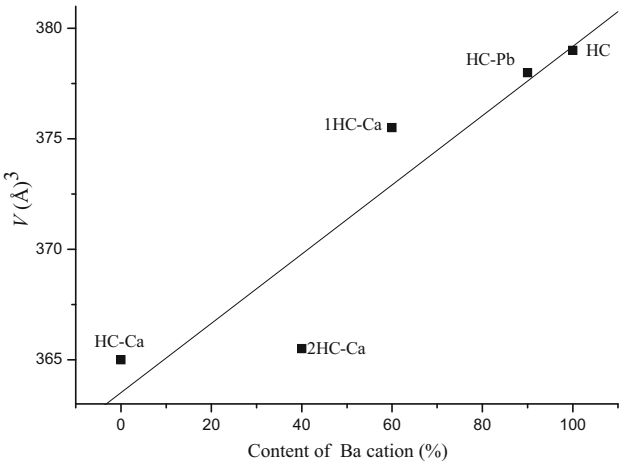

Fig. 2 Graph of the change the unit cell volume V, depending on the content of Ba^{2+} in the investigated hexacelsian, the HC-Ca is literature data (Dimitrijevic et al. 1996) (linear function for the curve $y = 364.88(1) + 0.14(2)\ r_i$, $r_i = 0.90$)

chemical formula $Ca_2Al_2SiO_7$ (Traore a et al. 2003). Gehlenite is a mineral that crystallizes in the tetragonal space group $_1m$ (Merlini et al. 2005), and structural motif is characterized by the existence of two tetrahedral layers.

3.2 Structural Analysis

The structures of Ca^{2+}-doped Ba-hexacelsian were refined in the space group $P\bar{3}c1$ with distinguishing positions of Si^{4+} and Al^{3+}. Structural model in space group $P\bar{3}c1$ was derived from model in space group $P6_3/mcm$ using group-subgroup relations and $P\bar{3}c1$ is maximal non-isomorphic subgroup of $P6_3/mcm$. The structure of Pb^{2+}-doped Ba-hexacelsian was refined in the space group $P6_3/mcm$ assuming disorder distribution of the Si^{4+} and Al^{3+}. Details relevant to the data collection and profile analyses of Ca^{2+}-, Pb^{2+}-doped Ba-hexacelsian are presented in Table 3.

3.2.1 Structure of Ba-Hexacelsian Doped with Ca^{2+} ion

In the structure of hexacelsian, the Ba^{2+} ions are located between layers of double six-member tetrahedral rings, coordinated with six equidistant oxygen (average interatomic length was 2.89 Å) and six more oxygen at a slightly larger distance (3.3 Å), CN = 12. During the ion-exchange process of $Ba^{2+} \rightarrow Ca^{2+}$, considering their respective ionic radii for coordination number 12 (for Ba^{2+} is 1.61 and for Ca^{2+} 1.34 Å), the calcium ion can replace only Ba^{2+} or take an interstitial position in the bulk or the grain boundaries.

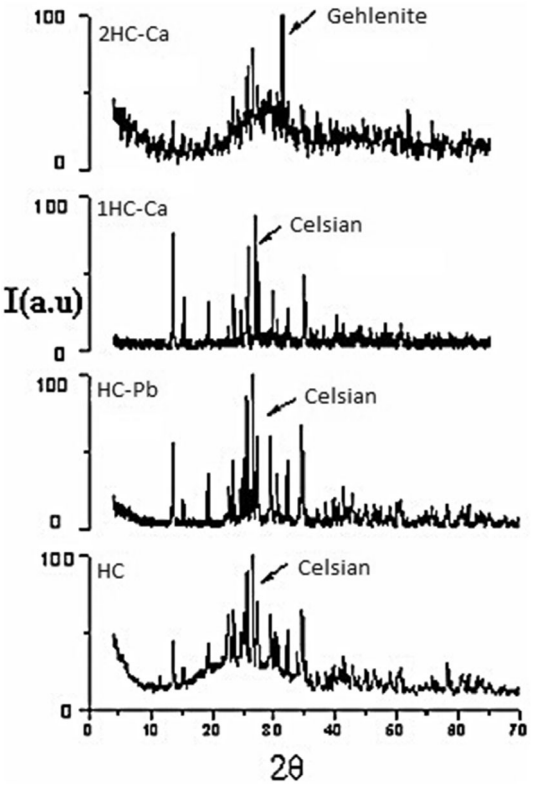

Fig. 3 The comparative XRPD diagrams of starting (HC) and ion-exchanged hexacelsian (HC-Pb, 1HC-Ca, 2HC-Ca) thermally treated in 1100 °C/1 h

The initial Rietveld refinement was carried out under the assumption that Ca^{2+} ions substituted for only Ba^{2+} ions in Wick of position 2*b*, space group $P6_3/mcm$. After refinement, the structure of doping hexacelsian with Ba^{2+} and Ca^{2+} in the position (0, 0, 0), in the difference-Fourier map, is appeared, the peak a significant electron density of 1.71 eÅ^3 and coordinate (0, 0, 0.1401). The part of extra framework cations in Ba-hexacelsian shows a significant displacement from special symmetry position 2*b* to Wick of position at 4*c*. For the oxygen in O_2 site, the difference-Fourier map shows an asymmetric electron-density distribution and higher temperature factor, Fig. 4a. To account

Table 3 Selected results from Rietveld refinements for samples of Ba-hexacelsian doped with Ca^{2+} and Pb^{2+}

	1HC-Ca	HC-Pb
Profile function type	TCH pseudo-Voigt	TCH pseudo-Voigt
Space group	$P\bar{3}c1$(165)	$P6_3/mcm$ (193)
Cell parameters	5.2995 (5)	5.2973 (5)
a (Å)	15.594 (4)	15.591 (4)
c (Å)	379.29 (3)	378.91 (3)
V (Å^3)	0.0034 (3)	0.00596 (3)
FWHM parameters	0.0197 (4)	0.01996 (3)
U	0.0018 (4)	0.04547 (3)
X	0.0972 (3)	0.08156 (3)
Y	0.0269 (4)	0.01361 (3)
Asy 1		
Asy 2		
Reliability factors	2.25	3.90
Chi^2		
R_{wp}	23.0	21.5
R_{exp}	15.3	15.0
R_p	19.9	19.0
R (F)	4.08	4.16
R (B)	5.74	4.50

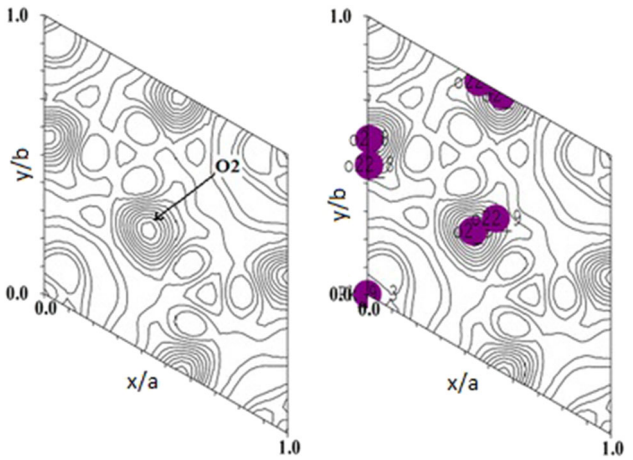

Fig. 4 **a** The oxygen in O_2 site, electron-density section at $z = 0$ for $0.0 \leq y \leq 1.0$ and $0.0 \leq x \leq 1.0$. **b** The anomalous feature is to arrange the oxygen in two positions: O_2 with coordinate (0.444; 0.0077; 0.1022) and O_2' (0.521; 0.0070; 0.1020)

for these anomalous features, the oxygen is arranged in two positions: O_2 with coordinate (0.444; 0.0077; 0.1022) and O_2' (0.521; 0.0070; 0.1020), Fig. 4b.

The difference-Fourier map showed the interatomic distances between peak for atom calcium and oxygen in position O_2' is 2.46 Å. This length bond corresponds to the Ca-O distance (2.41 Å), for Ca in coordination number 6 [rCa(VI) = 1.00Å]. According to this observation, we suppose that all or part of Ca^{2+} was placed in local symmetry at 4*c* site, in axis 3, with coordinates (0,0,*z*). The structure was refined with Ba^{2+} in position (0,0,0) and Ca^{2+} in (0,0,*z*) in space group $P\bar{3}c1$, with distinguishing positions of Si^{4+} and Al^{3+}. The occupations factor for position O_2 and O_2' was dependent on the ratio of extra framework cations Ba:Ca and is $O_2 : O_2' = 0.9: 0.1$. The final Rietveld refinement of hexacelsian doped with Ca^{2+} cation is presented in Fig. 5. In Table 4, refined fractional coordinates, atomic displacement parameters, Wick of position and site occupation factor (SOF) are presented.

The extra framework barium and calcium cations in symmetric position 2*b* and 4*c* (Fig. 6) are located in the structure of Ca^{2+}-doped diphylloaluminosilicate between each double layer. The coordination polyhedron around Ba and Ca are shown in Fig. 6. The atoms of barium are coordinated with 12 oxygen from the position of O_2 (Fig. 6).

The atom of Ca is coordinated with six oxygen in position O_2' (0.521, 0.0070, 0.1020), (see Fig. 7).

In the structure of doped hexacelsian, Ca cation forms three short and three long links with the average length of 2.417 and 2.903 Å. This approximately planar coordination for Ca cation is found in structures of mineral Ca-hexacelsian (Davis and Tuttle 1952; Daniel et al. 1995), anorthite *P* where one of the four cation positions for $Ca_{(000)}$ in the coordination 6 (Foit and Peacor 1973) and cation Ca in structure of Ca-LTA zeolite exists (Siegel et al. 1987).

3.2.2 *Structure of Ba-Hexacelsian Doped with Pb^{2+} ion*

The structure of Pb^{2+}-doped Ba-hexacelsian was refined in the space group $P6_3/mcm$ assuming disorder distribution of

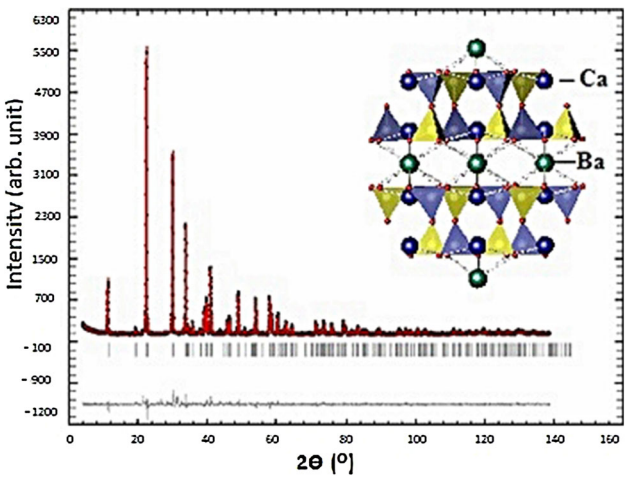

Fig. 5 Rietveld refinement patterns for Ca^{2+}-doped hexacelsian: the dots represent the observed intensities, and the solid line is the calculated one. A difference (obsd-calcd) plot is shown beneath

Table 4 Refined fractional coordinates (x, y, z), atomic displacement parameters (B_{iso}), Wick of position (W) and site occupation factor (SOF)

Atom	W	X	y	z	B_{iso}/Å^2	SOF
Ba	2*b*	0.0	0.0	0.0	0.979 (3)	0.1431 (2)
Ca	4*c*	0.0	0.0	0.1421(2)	0.979 (3)	0.022 (3)
Si1	4*d*	0.6666	0.3333	0.1459 (2)	1.443 (2)	0.333
Al1	4*d*	0.3333	0.6666	0.1438 (2)	1.443 (2)	0.333
O1	4*d*	0.3333	0.6666	0.2509 (1)	2.200 (2)	0.333
O_2	12 *g*	0.4444 (1)	0.0077 (1)	0.1022 (2)	2.447 (2)	0.90
O_2'	12 *g*	0.5391 (2)	0.0075 (1)	0.1026 (2)	2.447 (2)	0.10

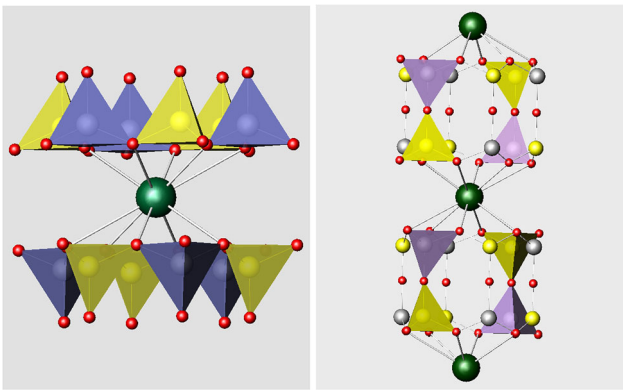

Fig. 6 **a** The coordination of Ba cation in the aluminosilicate network of hexacelsian; **b** coordination polyhedra around Ba cation in doped hexacelsian network. (green spheres represent the atoms Ba; SiO_4 tetrahedra are purple and yellow tetrahedra is AlO_4)

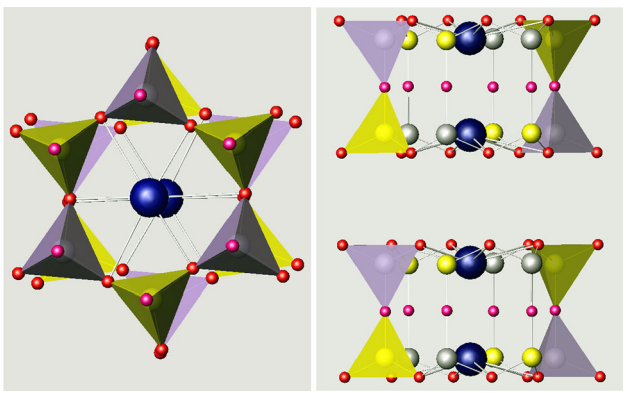

Fig. 7 **a** The coordination of Ca cation in the aluminosilicate network of hexacelsian; **b** coordination polyhedra around Ca cation in doped hexacelsian network. (blue spheres are Ca atoms; SiO_4 tetrahedra are purple and yellow tetrahedra is AlO_4)

the Si^{4+} and Al^{3+}(Kremenovic et al. 2003). The initial Rietveld refinement was carried out under the assumption that Pb^{2+} ions substituted for only Ba^{2+} ions in Wick of position 2*b*. Results of the Rietveld profile refinement of the sample $Ba_{0.90}Pb_{0.10}Al_2Si_2O_8$ are presented in Fig. 8. Fractional coordinates, atomic displacement parameters, Wick of position and site occupation factor (SOF) are presented in Table 5.

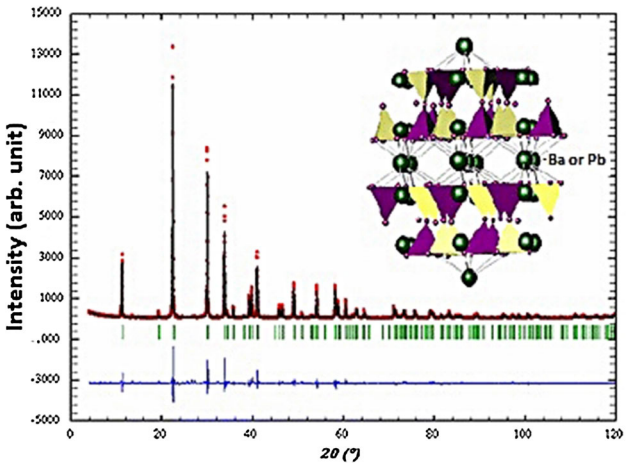

Fig. 8 Rietveld refinement patterns for Pb^{2+}-doped hexacelsian: The dots represent the observed intensities, and the solid line is the calculated one. A difference (obsd-calcd) plot is shown beneath

During the process of $Ba^{2+}\rightarrow Pb^{2+}$ ion change, the Pb^{2+} cation can replace Ba^{2+} cation in position 2*b*, because of the similar ionic radius for Ba^{2+} (for CN = 12; 1,61 Å) and Pb^{2+} (for CN = 12; 1,49 Å) (Shannon and Prewitt 1969). The distribution of Ba and Pb cations in the position (0,0,0) is not arranged, so it is relatively reserved high symmetry, Fig. 9.

The starting ratio Si/Al in LTA zeolite framework was Si:Al = 1:1. If you ignore the impact of extra framework cations, in TO_4 tetrahedra calculated interatomic distance for Si − O bond from Shanan radius is 1.61 and for Al–O length bond is 1.74 Å (for O^{-2} in coordination II) (Shannon and Prewitt 1969). Calculated average interatomic distance (Si, Al)–O for atomic ratio Si: Al = 1: 1 must be at 1.675 Å (Smith 1974). The values for interatomic < T–O > distance, after the process doping in the structure of hexacelsian, are 1.670 for Ca^{2+}—hexacelsian and 1.668 for Pb^{2+}-hexacelsian. Based on the literature data (Kremenovic et al. 2003; Shannon and Prewitt 1969; Smith 1974), we can make a curve showing the linear dependence of length bond <T–O> and Si content (%) in the aluminosilicate network of hexacelsian, Fig. 10.

Table 5 Refined fractional coordinates (x, y, z), atomic displacement parameters (B_{iso}/Å^2), Wick of position (W) and site occupation factor (SOF)

Atom	W	x	y	z	B_{iso}/(Å^2)	SOF
Ba	2*b*	0.0	0.0	0.0	1.306 (3)	0.158 (2)
Pb	2*b*	0.0	0.0	0.0	1.306 (3)	0.007 (3)
Si1	4*d*	0.6666	0.3333	0.1468 (2)	1.447 (2)	0.167
Al1	4*d*	0.3333	0.6666	0.1438 (2)	1.447 (2)	0.167
O1	4*d*	0.6666	0.3333	0.2494 (1)	2.615 (2)	0.167
O_2	12 *g*	0.4445 (3)	0.0073	0.1030 (2)	2.447 (2)	0.50

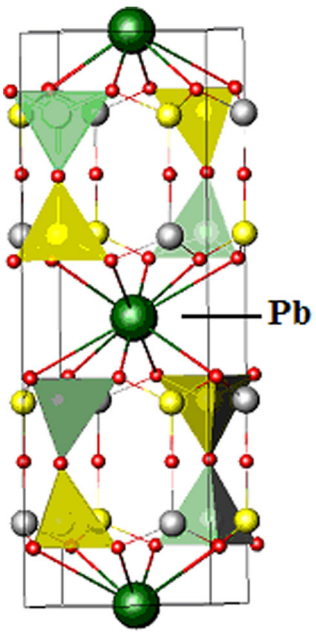

Fig. 9 The coordination polyhedra of structure $Ba_{0.9}Pb_{0.1}Al_2Si_2O_8$ (green spheres represent the atoms Ba or Pb; SiO_4 tetrahedra are yellow and purple tetrahedra is AlO_4)

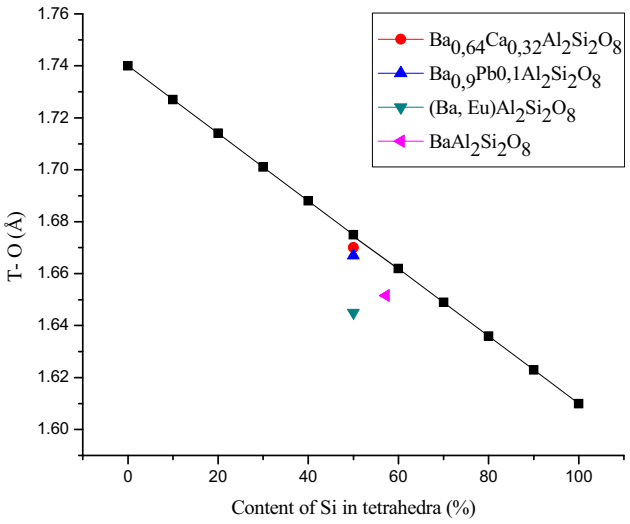

Fig. 10 The graphic of bond length <T–O> in the hexacelsian doped with Eu s.g. *P6*$_3$*/mcm* (McKittrick et al. 1996) α-hexacelsian s.g. P (Im et al. 2006), Ba, Ca-hexacelsian p.g $P\bar{3}c1$, Ba, Pb-hexacelsian p.g. *P6*$_3$*/mcm*

The value of average bond length <T–O> for doped hexacelsian in space group $P\bar{3}c1$ is close to calculated value. This indicates that this space group, with separate tetrahedral positions for Si and Al, is probably the best for the refinement of structure hexacelsian. Calculated average <T–O> distances for both samples are 1.670 for Ca^{2+}-doped and 1.668 for Pb^{2+}-doped hexacelsian, this indicates that the starting ratio of Si/Al remains after ion-doped process. Presence of the doped cations Ca^{2+} and Pb^{2+} in structure of hexacelsian does not have a significant effect on the length bonds of (Si, Al)–O in the aluminosilicate framework.

The interatomic distance M–O (M = Ba^{2+}, Ca^{2+}, Pb^{2+}) in the structure of doped hexacelsian is presented in Table 7. The calculated bond length for M–O [M = Ba^{2+}, Ca^{2+} and Pb^{2+}] a basis of Sanon radius was: Ba–O = 3.01 Å, Pb–O = 2.89 Å, if CN = 12; Ca–O = 2.40 Å if CN = 6 (Foit and Peacor 1973). The experimental values for doped hexacelsian match are calculated as shown in Table 6.

The calculated bond length for M–O [M = Ba^{2+}, Ca^{2+} and Pb^{2+}], a basis of Shanan radius (Shannon and Prewitt 1969), was: Ba–O = 3.01 Å, Pb–O = 2.89 Å, if CN = 12; Ca–O = 2.40 Å if CN = 6 (Siegel et al. 1987). The experimental values for doped hexacelsian are in good agreement with calculated ones [for Ca^{2+}-doped hexacelsian the average distances are <Ba–O> = 3.09, <Ca–O> and for Pb^{2+}-doped hexacelsian is 3.105]. The average distance of M–O (M = Ba^{2+}, Sr^{2+}, Pb^{2+}) and bond valence

Table 6 The interatomic distance M–O (M = Ba^{2+}, Ca^{2+}, Pb^{2+}) (Å) in the structure of doped hexacelsian

1HC–Ca		HC–Pb
M–O (Å)		
Ba–O_2	6 × 2.82 (2)	6 × 2.84 (2)
	6 × 3.36 (2)	6 × 3.37 (2)
<Ba–O>	3.09	3.105
Ca–O_2'	3 × 2.90 (1)	–
	3 × 2.41 (1)	–
<Ca–O>	2.66	–
<M–O>	2.875	3.105

Table 7 The bond length for M–O and i bond valence sum ($\sum v_{ij}$) for experimental and literature data of hexacelsian

Formula	Hexacelsian* $BaAl_2Si_2O_8$	α-hexacelsian β-hexacelsian** $BaAl_2Si_2O_8$		Hexacelsian*** $BaAl_2Si_2O_8$	1-HC-Ca $Ba_{0.64}Ca_{0.32}Al_2Si_2O_8$	HC-Pb $Ba_{0.9}Pb_{0.1}Al_2Si_2O_8$
p.g.	*P*6/mmm (191)	P $\bar{3}$(147)		*P*6$_3$/*mcm* (193)	*P*$\bar{3}$*c*1 (165)	*P*$\bar{3}$*c*1 (165)
Ba–O_2	6 × 2.885 6 × 3.335	6 × 2.878 (4) 6 × 3.325 (5)	6 × 2.895 (6) 6 × 3.373 (6)	6 × 3.052 (1) 6 × 3.151 (1)	6 × 2.82 (2) 6 × 3.36 (2)	6 × 2.84 (2) 6 × 3.37 (2)
<M–O>	3.11	3.101	3.134	3.101	3.091	3.105
$\sum v_{ij}$–M	1.674	1.704	1.596	1.452	1.792	1.806

*Ito (1950)

**Kremenović et al. (1997)

**Takéuchi (1958)

sum for doped hexacelsian, as in the literature data (Kremenović et al. 1997, 2003; Takéuchi 1958), are presented in Table 6. The bond valence sum is a popular method to estimate the oxidation states and coordination geometries of atoms (Urusov 2004).

Calculated data for the bond valence sum $\sum v_{ij}$–M showed the low value ranging from 1.452 to 1.596 for hexacelsian (Table 7) and indicates the presence of disorder as well as oxygen vacancy in the crystallographic position (0, 0, 0) in the investigated hexacelsian. The disorder is very weak in the samples where the hexacelsian ion exchanged with Ca and Pb cations 1-HC-Ca ($\Sigma v_{ijj} = 1866$) i HC-Pb ($\Sigma v_{ij} = 1806$). The calculated values for the sum of valency bond indicate that the coordination sphere of M-cations takes all 12 of oxygen at the O_2 position, i.e., the M-cation NC = 12. The six long interatomic distances for 1-HC-Ca (6 × 3.36 Å) and for HC-Pb (6 × 3.37 Å) generally have small influence related to the total valency of ion-changed hexacelsian, while for hexacelsian doped with Eu that influence is important (Im et al. 2006).

4 Conclusion

Ba-diphylloaluminosilicates were doped with Ca^{2+} and Pb^{2+} ions by the ion-exchange procedure. Rietveld refinement results clearly indicate that Ca^{2+} and Pb^{2+} ions are incorporated into the hexacelsians structure. The structure of Ca^{2+}-doped Ba-hexacelsian was refined in the space group *P*$\bar{3}$*c*1 which distinguishes the positions of Si^{4+} and Al^{3+}. The structural analysis showed that the Ca atom is incorporated between each double layer in symmetric position 2*b* and 4*c*. The Ca atoms have an approximately planar coordination and are coordinated with six oxygen in position O_2'. The structure of Pb^{2+}-doped Ba-hexacelsian was refined in the space group *P*6$_3$/*mcm* assuming disorder distribution of the Si^{4+} and Al^{3+}. The initial Rietveld refinement was carried out under the assumption that Pb^{2+} ions are substituted only Ba^{2+} ions in Wick of position 2*b*. The different atomic positions of Ca and Pb in hexacelsian are probably due to the different ionic radius. The average interatomic length between the Ca^{2+} ion and oxygen is less than interatomic bond distances between the Pb^{2+} ion and oxygen. Calculated data for the bond valence sum $\sum v_{ij}$-M indicate disordering and oxygen vacancy in the crystallographic position (0, 0, 0) in the investigated hexacelsian.

Acknowledgements The authors are grateful for financial support of the Ministry of Education, Science and Technology of the Republic of Serbia (Project Number III-45,012).

References

Colomban PH, Courret H, Romain F, Gouadec G, Michel D (2000) Sol-gel-prepared pure and lithium-doped hexacelsian polymorphs: an infrared, Raman, and thermal expansion study of the beta-phase stabilization by frozen short-range disorder. J Am Ceram Soc 83(12):2974–2982

Daniel I, Gillet P, McMillan PF, Richet P (1995) An in situ high-temperature structural study of stable and metastable $CaAl_2Si_2O_8$ polymorphs. Mineral Mag 59:25–33

Davis GL, Tuttle OF (1952) Two new crystalline phases of the anorthite composition $CaO.Al_2O_3.Si0_2$. Amer J Sci Bowen 250:107–114

Dimitrijević R, Dondur V, Kremenović A (1996) Thermally induced phase transformation of Ca-exchanged LTA and FAU zeolite frameworks: rietveld refinement of the hexagonal $CaAl_2Si_2O_8$ diphyllosilicate structure. Zeolites 16:294–300

Dondur V, Dimitrijevic R, Kremenovic A, Damjanovic Lj, Kicanovic M, Cheong HM, Macura S (2005) Phase transformation of hexacelsians doped with Li, Na and Ca. Mater Sci Forum 494:107–112

Dondur V, Dimitrijevic R, Kremenovic A, Damjanovic LJ, Romčević N, Macura S (2008) The lithium- and sodium-enhanced transformation of Ba-exchanged zeolite LTA into celsian phase. J Phys Chem Solids 69:2827–2832

Dyer A (1998) Ion-exchange capacity. In: Robson H (ed) Verified Synthesis of Zeolite Materials. Microporous Materials, vol 22, p 543

Ferone C, Esposito S, Dell'Agli G, Pansini M (2005) Role of Li in the low temperature synthesis of monoclinic celsian from (Ba, Li)-exchanged zeolite—a precursor. Solid State Sci 7:1406–1414

Foit FF, Peacor DR (1973) The anorthite crystal structure at 410 and 830 °C. Am Mineral 58:665–675

Im BW, Kim YI, Jeon YD (2006) Thermal stability study of $BaAl_2Si_2O_8:Eu^{2+}$ phosphor using its polymorphism for plasma display panel application. Chem Mater 18(5):1190–1195. doi:10.1021/cm051894v

Isaacs TJ (1971) Fluorescence of Alkaline-Earth Silicates Activated with divalent europium. J Electrochem Soc Solid State Sci 118 (6):1009–1111

Ishihara T, Tanaka T, Hirao K, Soge N (1997) Fracto-luminescence of rare earth element-doped hexacelsian ($BaAl_2Si_2O_8$). Jpn J Appl Phys 36:L781

Ishihara T, Tanaka T, Fujita K, Hiraob K, Sogab N (1998) Full color triboluminescence of rare-earth-doped hexacelsian ($BaAl_2Si_2O_8$). Solid State Commun 107(12):763–767

Ito T (1950) Alpha-Celsian. X-ray studies on polymorphism. Maruzen, Tokyo, pp 19–29

Kim C, Kwon I, Park C et al (2000) Phosphors for plasma display panels. J Alloys Compd 311:33

Kim YL, Im WB, Jeon DY (2006) Combined Rietveld refinement of $CaMgSi_2O_6:Eu^{2+}$ using X-ray and neutron powder diffraction data. Chem Mater 18:1190–1195

Kremenović A, Norby P, Dimitrijević R, Dondur V (1997) Time-temperature resolved synchrotron XRPD study of the hexacelsian alpha ↔ beta polymorph inversion. Solid State Ion 101–103:611–618

Kremenović A, Colomban Ph, Piriou B, Massiot D, Florian P (2003) Structural and spectroscopic characterization of the quenched hexacelsian. J Phys Chem Solids 64(11):2253–2268

Libay F (1985) Structural chemistry of silicates. Springer-Verlag, Berlin

McKittrick J, Hoghooghi B, Lopez OA (1996) Vitrification and crystallization of barium aluminosilicate glass ceramics from zeolite precursors. J Non Cryst Solids 197(2–3):170–178

Merlini M, Gemmi M, Artioli G (2005) High-pressure behavior of åkermanite and gehlenite and phase stability of the normal structure in melilites. Phys Chem Miner 32:189–196

Nedić B, Dondur V, Kremenović A, Dimitrijevic R, Blanuša J, Vasiljević-Radović D, Stoiljković M (2007) Yb^{3+} doped dyphillosilicates prepared by thermally induced phase transformation of zeolites. Russ J Phys Chem A 81(9):1413–1417

Radosavljevic-Mihajlovic A, Prekajski M, Zagorac J, Došen A, Nenadović S, Matović B (2012) Thermal transformation of Ba-exchanged A and X zeolites into monoclinic celsian. Cera Int 38 (3):2347–2354

Rodriguez-Carvajal J, Roisnel T (1998) Full Prof.98 and WinPLOTER new windows applications for diffraction commission on powder diffraction. IUCr Newsletter

Shannon RD, Prewitt CT (1969) Effective ionic radii in oxides and fluorides. Acta Crystallogr B25:925–945

Siegel H, Schoellner R, Staudte B, van Dun JJ, Mortier WJ (1987) X-ray structural investigations on hydrothermally treated (Ca_4, Na_4)-A zeolites. Zeolites 7:372–378

Sinha K, Pearson B, Casolco SR, Garay JE, Graeve OA (2009) Synthesis and consolidation of $BaAl_2Si_2O_8$:eu: development of an integrated process for luminescent smart ceramic materials. J Am Ceram Soc 92:2504–2511

Smith JV (1974) Feldspar minerals. Crystal structure and physical properties, vol 1. Springer-Verlag, Berlin, Heidelberg

Tabira Y, Withers RL, Takéuchi Y, Marumo F (2000) Structured diffuse scattering, displacive flexibility and polymorphism in Ba-hexacelsian. Phys Chem Miner 27(3):194–202

Takéuchi Y (1958) A detailed investigation of the structure of hexagonal $BaAl_2Si_2O_8$ with reference to its α–β inversion. Mineral J 2(5):311–332

Takéuchi Y, Donnay G (1959) The crystal structure of hexagonal $BaAl_2Si_2O_8$. Acta Crystallogr A 12:465–470

Talin A, Dean K, Jaskie J (2001) Field emission displays: a critical review. Solid State Electron 45:963–976

Traore K, Kabre TS, Blanchartb P (2003) Gehlenite and anorthite crystallisation from kaolinite and calcite mix. Ceram Int 29:377–383

Urusov VS (2004) Principles and criteria for the choice and refinement of structural models in inorganic crystal chemistry. Crystallogr Rep 49(4):559–572

Yoshiki B, Matsumoto K (1951) High-temperature modification of barium feldspar. J Am Ceram Soc 34(9):283–286